The Journal of Immunology

Distinct Host–Mycobacterial Pathogen Interactions between Resistant Adult and Tolerant Tadpole Life Stages of *Xenopus laevis*

Kun Hyoe Rhoo, Eva-Stina Edholm, María J. Forzán, Adil Khan, Anthony W. Waddle, Martin S. Pavelka, Jr. and Jacques Robert

J Immunol published online 7 October 2019
http://www.jimmunol.org/content/early/2019/10/04/jimmunol.1900459

The Journal of Immunology is published twice each month by
The American Association of Immunologists, Inc.,
1451 Rockville Pike, Suite 650, Rockville, MD 20852

Print ISSN: 0022-1767 Online ISSN: 1550-6606.

Published October 7, 2019, doi:10.4049/jimmunol.1900459

Distinct Host–Mycobacterial Pathogen Interactions between Resistant Adult and Tolerant Tadpole Life Stages of *Xenopus laevis*

Kun Hyoe Rhoo,* Eva-Stina Edholm,† María J. Forzán,‡ Adil Khan,* Anthony W. Waddle,*,§ Martin S. Pavelka, Jr.,* and Jacques Robert*

Mycobacterium marinum **is a promiscuous pathogen infecting many vertebrates, including humans, whose persistent infections are problematic for aquaculture and public health. Among unsettled aspects of host–pathogen interactions, the respective roles of conventional and innate-like T (iT) cells in host defenses against *M. marinum* remain unclear. In this study, we developed an infection model system in the amphibian *Xenopus laevis* to study host responses to *M. marinum* at two distinct life stages, tadpole and adult. Adult frogs possess efficient conventional T cell–mediated immunity, whereas tadpoles predominantly rely on iT cells. We hypothesized that tadpoles are more susceptible and elicit weaker immune responses to *M. marinum* than adults. However, our results show that, although anti–*M. marinum* immune responses between tadpoles and adults are different, tadpoles are as resistant to *M. marinum* inoculation as adult frogs. *M. marinum* inoculation triggered a robust proinflammatory $CD8^+$ T cell response in adults, whereas tadpoles elicited only a noninflammatory CD8 negative- and iT cell–mediated response. Furthermore, adult anti–*M. marinum* responses induced active granuloma formation with abundant T cell infiltration and were associated with significantly reduced *M. marinum* loads. This is reminiscent of local $CD8^+$ T cell response in lung granulomas of human tuberculosis patients. In contrast, tadpoles rarely exhibited granulomas and tolerated persistent *M. marinum* accumulation. Gene expression profiling confirmed poor tadpole $CD8^+$ T cell response, contrasting with the marked increase in transcript levels of the anti–*M. marinum* invariant TCR rearrangement (*iVα45-Jα1.14*) and of CD4. These data provide novel insights into the critical roles of iT cells in vertebrate antimycobacterial immune response and tolerance to pathogens.** ***The Journal of Immunology*****, 2019, 203: 000–000.**

Mycobacterium marinum resides in marine and fresh water and is capable of infecting a broad range of aquatic species including fish, reptiles, amphibians [e.g., *Xenopus laevis* (1)], and mammals including humans (reviewed in Ref. 2). *M. marinum* is difficult to eradicate in aquaculture, especially when introduced to a recirculating water system. This pathogen, which causes fish mycobacteriosis outbreaks, can severely impact aquaculture, as reviewed in Ref. 3. In humans, *M. marinum* causes opportunistic infection in the skin and poses public health risks (3). As such, a better understanding of host immune responses to *M. marinum* remains crucial to improve diagnostics, treatment options, and vaccine strategies.

Importantly, *M. marinum* often serves as a useful Biosafety Level 2 alternative pathogen for *M. tuberculosis*, the causative agent for important human tuberculosis (4). Like *M. tuberculosis*, *M. marinum* has been shown to survive within host macrophages and is able to induce caseating granulomas in a zebrafish model (5). Furthermore, studies have shown that *M. tuberculosis* and *M. marinum* share selected virulence determinants such as ESX-1 secretion system for phagosomal arrest in the host macrophages (1). *M. marinum* grows optimally at 30–33°C, which is lower than the optimal temperature of *M. tuberculosis* (~37°C) and replicates every 4 hours, which is markedly shorter than the replication time of *M. tuberculosis* (~20 hours) and more convenient for in vitro studies. Therefore, investigation with *M. marinum* will further benefit our understanding of host antimycobacterial immune responses, providing a valuable and practical model that may ultimately lead to the development of new immunotherapeutic-based strategies for tuberculosis.

X. laevis is an attractive comparative immunology animal model because of its fully sequenced genome and the availability of large genetic and genomic resources, as well as the remarkable similarity of its immune system to that of humans (6, 7). Unlike mammals, however, *X. laevis* undergoes metamorphosis and has distinct T cell populations prior to and after this developmental transition. *X. laevis* tadpoles lack an optimal protein level of classical MHC class I (MHC I) molecules yet express multiple *Xenopus* MHC I–like genes. In mammals, MHC I–like molecules have been shown to restrict innate-like T (iT) cells that exhibit

*Department of Immunology and Microbiology, University of Rochester, Medical Center, Rochester, NY 14642; †Norwegian College of Fishery Science, University of Tromsø, N-9037 Tromsø, Norway; ‡Cornell Wildlife Health Lab, Animal Health Diagnostic Center, College of Veterinary Medicine, Cornell University, Ithaca, NY 14850; and §One Health Research Group, Melbourne Veterinary School, The University of Melbourne, Werribee, Victoria 3030, Australia

ORCIDs: 0000-0002-0810-9911 (M.J.F.); 0000-0002-0717-3268 (A.K.); 0000-0002-5154-4302 (A.W.W.); 0000-0003-3265-8555 (M.S.P.).

Received for publication April 23, 2019. Accepted for publication September 16, 2019.

This work was supported by a predoctoral fellowship (T32AI118689 to K.H.R.), as well as R21AI139718 and R24AI059830, all from the National Institute of Allergy and Infectious Diseases, National Institutes of Health, and IOS-1456213 from the National Science Foundation.

Address correspondence and reprint requests to Dr. Jacques Robert, Department of Microbiology and Immunology, University of Rochester Medical Center, 601 Elmwood Avenue, Rochester, NY 14642. E-mail address: Jacques_Robert@urmc.rochester.edu

Abbreviations used in this article: CT, cycle threshold; dpi, day postinfection; IHC, immunohistochemical/immunohistochemistry; iNOS, inducible NO synthase; isH, in situ hybridization; iT, innate-like T; iVα45, invariant Vα45; iVα45-Jα1.14, invariant Vα45-Jα1.14; MHC I, MHC class I; PL, peritoneal leukocyte; qPCR, quantitative PCR; qRT-PCR, quantitative RT-PCR; Treg, regulatory T cell.

features of both innate and adaptive immune cell effectors. Similarly, several iT cell subsets have been identified in *X. laevis* (8). These iT cell subsets are predominant in tadpoles, representing as much as 80% of $CD8^{low/negative}$ splenic T cells, whereas they represent only a minority compared with conventional T cells in adult *X. laevis*.

Generally, tadpoles are considered to have a less efficient immune response and, thus, to be more susceptible to natural pathogens (reviewed in Ref. 7). However, a more detailed investigation in *X. laevis* suggests that distinct specialization of immune response mediated by iT cells allows the immune competence of tadpoles against distinct pathogens (9, 10). Importantly, one of the iT cell populations exhibiting the invariant TCRα rearrangement *iVα45-Jα1.14* has been shown to be critical for tadpole resistance to *M. marinum* infection (10).

In mammalian models, two iT cell subsets have been studied in the context of antimycobacterial immune response: mucosal-associated innate T cells and invariant NKT cells. A few clinical studies, along with in vitro studies, suggest protective functions of both types of iT cell, at least at the early stage of mycobacterial infections (reviewed in Refs. 11, 12). However, investigation of the specific regulatory and/or effector functions, activation, and recruitment of iNKT and mucosal-associated innate T cells has been challenged by the lack of suitable animal models (reviewed in Ref. 13). As such, *X. laevis*, exhibiting a distinct T cell balance between different life stages, would provide a useful model system to gather new insights into iT cell–mediated immune functions during mycobacterial infection.

In this study, we report evidence of a distinct immune response and histopathologic condition between *X. laevis* adults and tadpoles toward *M. marinum*. In support of our hypothesis that the respective response of iT and conventional T cells is distinct between tadpoles and adult frogs, we found markedly different conventional anti–*M. marinum* T cell responses, histopathology, and *M. marinum* growth between these two life stages.

Materials and Methods

Animals

Two-year-old adult frogs and 3-wk-old premetamorphic outbred tadpoles (stage 52) were obtained from our *X. laevis* research resource for immunology at the University of Rochester (Rochester, NY; https://www.urmc.rochester.edu/microbiology-immunology/xenopus-laevis.aspx). During experiments, all animals were carefully handled under University of Rochester Committee on Animal Resources regulations (approval no. 100577/2003-151).

M. marinum *inoculation*

The *M. marinum* strain PM2960 was derived from a clinical isolate (stock no. PM2690) generously provided by Dr. D. Hardy (University of Rochester). Fluorescent *M. marinum* strain PM3495 was generated by transformation of a plasmid (pMV261.Kan.DsRed), kindly provided by W. R. Jacobs (Albert Einstein College of Medicine, Bronx, NY), into the parental PM2960 strain of *M. marinum*. *M. marinum* was cultured in Middlebrook 7H9 broth until saturation, and titered stocks were prepared and frozen at −80°C as previously described (10). A working concentration for i.p. injection into the animals and for in vitro infection of leukocytes was prepared by diluting the growth media in the amphibian PBS with 0.05% Tween 80. Tissues were harvested from euthanized animals at indicated days postinoculation or from postmortem animals for further analyses.

Survival analysis of M. marinum*–inoculated adults and tadpoles*

To examine the host resistance of *X. laevis* adults and tadpoles to *M. marinum* infection, 4-mo-old adult frogs and 3-wk-old premetamorphic tadpoles (stage 52) (14) were i.p. inoculated with three different doses of *M. marinum*: low dose (5×10^5 CFU), medium dose (1×10^6 CFU), and high dose (2×10^6 CFU). The survival of the animals was monitored daily for 1 mo, and we investigated the effects of host life stage (tadpole or adult) and dose on survivorship.

Histopathology, immunohistochemistry, and in situ hybridization

The livers of postmortem adult frogs (euthanized at 14 and 50 d postinfection [dpi], $n = 1$ each) and whole tadpoles (euthanized at 30 dpi, $n = 2$) inoculated with *M. marinum* were fixed in 10% formalin and processed for routine histologic examination. Based on previous observation, the liver serves as the main organ infected by *M. marinum* (10). Cross-sections of the adult livers and full-length longitudinal sections of the tadpoles were stained with H&E (15) as well as special stains for bacteria and acid-fast organisms: Gram (16), Ziehl Neelsen (15), and Fite Faraco (17). Microgranulomas were counted in three random low-power fields (×10) from four adults (50 dpi) and four tadpoles (30 dpi). The average number of microgranulomas per individual was used to represent the number of microgranulomas per 0.5 mm^2 of liver tissue. Immunohistochemical (IHC) staining with anti-CD3 receptor Ab [catalog no. PA0553; Leica (18)] was performed using an automated platform to identify conventional T cells (Bond-Max IHC/ISH platform, Bond Polymer Refine DAB kit, and Bond Polymer Refine Red kit; Leica Biosystems, Newcastle upon Tyne, U.K.). A negative control (staining without the primary anti-CD3 staining) was run along with the test slides. A tissue was considered positive if strong and distinct staining with anti-CD3 Ab was present in the membrane of individual cells and background staining was either absent or clearly distinct from true specific staining. An in situ hybridization (isH) probe for *Mycobacterium* sp. (ACDBio RNAscope Probe-B-MBovis-23S rRNA, catalog no. 446011, Target region 3-3 – 1286, GenBank NR_076088.1) was applied following the manufacturer's specifications to identify the presence of *M. marinum*.

RNA and genomic DNA isolation from tissues, RT-PCR, and PCR

Total RNA and genomic DNA were extracted from the animals' tissues using TRIzol reagent, following the manufacturer's protocol (Invitrogen). A total of 2 μg of RNA was used to synthesize cDNA by a reverse transcriptase, M-MLV (Invitrogen), with a mixture of oligo(dT) primers (Invitrogen). For RT-PCR, 125 ng of cDNA was used to determine the expression levels of genes of interest by ΔΔ cycle threshold (Ct) value with an ABI 7300 Real-Time PCR System and PerfeCTa SYBR Green FastMix ROX. The expression levels are normalized to that of an endogenous housekeeping gene, *gapdh*, and then further normalized against the lowest observed expression. All the primers are validated prior to use. Furthermore, the absolute quantification method was done using the quantitative RT-PCR (qRT-PCR) analysis. An *M. marinum* 16S rRNA PCR fragment was cloned into the pGEM-Easy Vector (Promega) and further transformed into DH10β competent bacteria for amplification. The plasmid stock was serially diluted in the range between 10^{10} and 10^1 plasmid copies of 16S rRNA *M. marinum* to generate a standard curve by absolute qRT-PCR. To determine *M. marinum* loads, a total of 250 ng of genomic DNA was used as a template, and then the absolute copy number of *M. marinum* 16S rRNA genome was extrapolated from the standard curve. All primer sequences are listed in Table I.

Statistical analysis

For studying the kinetics of *M. marinum* loads, a nonparametric Kruskal–Wallis test followed by Dunn test for multiple comparisons was performed. For RNA expression analyses, a mixed linear regression model analysis was performed to compare the kinetics of adults and tadpoles, followed by the Kruskal–Wallis test to compare individual time points within adult or tadpole groups. For the survival analysis, a log-rank test and the Cox proportional hazard model analysis were performed using R (R version 3.5.2, RStudio version 1.1.463). GraphPad Prism 6 software (San Diego, CA) was used for all statistical computation except for Cox proportional hazard model analysis.

Results

Comparison of survival rates following M. marinum *inoculation between* X. laevis *adults and tadpoles*

To examine the respective host resistance of tadpoles and adult frogs to *M. marinum*, we monitored survival and bacterial loads (Table I) following different doses of *M. marinum* inoculation. Although tadpole death appeared to start earlier than adult death for low and medium *M. marinum* doses (Fig. 1), the mortality

Table I. List of qPCR primer sequences

Primer	Sequence (5′-3′)
CCR2	F: 5′-ATTGGGCAGAACTGTGGTAG-3′
	R: 5′-GGGCGAGTAATCTGAGTCATAA-3′
CD3	F: 5′-TTGGGCTCAGTGTGGAATG-3′
	R: 5′-GGTCCCGGTATCCATCTCTAT-3′
CD4	F: 5′-CATAGTGGTTTCCCTCTGGTTTAG-3′
	R: 5′-CGCAGAGCGTCCATTCATTA-3′
CD8β	F: 5′-GGAACACGTTTACCCTGAAGA-3′
	R: 5′-GGGAGGTTCCATTCCCAAAT-3′
CSF-R1	F: 5′-TGTATTCTTTGGACTTGCCGTATCTGG-3′
	R: 5′-TTGTTTAGCTTCAAATTCTGGGTAATA-3′
GAPDH	F: 5′-GACATCAAGGCCGCCATTAAGACT-3′
	R: 5′-AGATGGAGGAGTGAGTGTCACCAT-3′
G-CSF-R	F: 5′-ACGTGCCAGCTAAACCTCACAGAT-3′
	R: 5′-TGACACAGCCTGGGCGAGAAATAA-3′
IL-1β	F: 5′-CATTCCCATGGAGGGCTACA-3′
	R: 5′-TGACTGCCACTGAGCAGCAT-3′
IL-10	F: 5′-TGCTGGATCTTAAGCACACCCTGA-3′
	R: 5′-TGTACAGGCCTTGTTCACGCATCT-3′
iNOS	F: 5′-AACCGTAAGCCAAAGAAGGA-3′
	R: 5′-TGGTTCTGGCAGCCACAGT-3′
M. marinum 16S rRNA	F: 5′-AGAGTTTGATCCTGGCTCAG-3′
	R: 5′-CACTCGAGTATCTCCGAAGA-3′
TGF-β	F: 5′-CCCACAGGCCAAAGATATAGAC-3′
	R: 5′-CATCAGGTAGGGTTTCGTGTT-3′
TNF-α	F: 5′-TGTCAGGCAGGAAAGAAGCA-3′
	R: 5′-CAGCAGAGCAAAGAGGATGGT-3′
	R: 5′-CCGACACACTGAGCGGAAA-3′
Vα45-Jα1.14	F: 5′-TCCGTTAACGAGAAGGATTCCCAG-3′
	R: 5′-CTCCCAGCCACTACCAGAATAAG-3′

F, forward; iNOS, inducible NO synthase; R, reverse.

rate was not statistically different using a log-rank test. To substantiate our analysis, we tested our data using a final statistical model and set different *M. marinum* doses and two life stages (adults and tadpoles) as covariates. The analysis indicates that survivorship was not significantly impacted by life stage ($p = 0.1357$); instead, survivorship appeared to be *M. marinum* dose–dependent. The interaction between life stage and dose was nonsignificant in our initial model. Furthermore, survivorship decreased with increasing *M. marinum* dose: medium and high doses both had significantly lower survivorship than low dose ($p = 0.0404$ and $p < 0.0001$, respectively), and high dose had significantly lower survivorship than medium dose ($p < 0.0001$). The median survival time for each dose is indicated in Table II. Collectively, our survival analysis suggests that tadpoles are not significantly more susceptible against *M. marinum* compared with adult frogs.

We also quantified the *M. marinum* genome copy number of postmortem animals by quantitative PCR (qPCR) (Fig. 1B, 1C). Relatively modest *M. marinum* loads were detected in tissues of postmortem adult frogs (10–100-fold higher in respective tissues of postmortem animals compared with live animals euthanized at 21 dpi). These *M. marinum* loads were not significantly different across organs or at different times of death (Fig. 1B). Similarly, there was no correlation ($p = 0.9738$ by Spearman r analysis) between the total *M. marinum* loads in tadpoles and time of death. The rapid decay of tadpoles dying from *M. marinum* inoculation did not allow the determination of the bacterial loads for particular organs without a risk of contamination.

Comparison of T cell–mediated immune responses in X. laevis *adults and tadpoles*

To address our hypothesis that adults and tadpoles have distinct T cell responses during *M. marinum* infection, we performed flow cytometry using *Xenopus*-specific anti-CD8 mAb and anti-CD5 mAb to define the response kinetics of two main T cell populations as previously established using adult splenocytes (19): a $CD8^+$ T cell population, defined as cells coexpressing the CD8 and CD5 pan–T cell marker ($CD8^+/CD5^+$), and a $CD5^+$ T cell population not significantly expressing CD8 ($CD8^{neg}/CD5^+$) that includes iT cells and presumably CD4 T cells and that we will refer to in this article as a $CD8^{neg}$ T/iT cell population (Fig. 2A, 2B). In the absence of lymph nodes, the spleen constitutes both a primary and secondary lymphoid organ in *Xenopus* (20). Therefore, we monitored the kinetics of the two T cell subsets in the spleen (Fig. 3). We also examined the liver, which is a major site of mycobacterial infection in *Xenopus* (Fig. 4).

In adult frogs, but not in tadpoles, there was an increase of the total number of splenocytes upon *M. marinum* inoculation, which reached statistical significance at 21 dpi, suggestive of immune cell expansion (Table III). Notably, the frequency and the number of CD8 T cells were significantly increased in the adult spleens at 12 dpi (***$p = 0.001$ compared with the 6-dpi group; **$p = 0.0154$ compared with the uninfected group), whereas no significant change was observed in tadpoles (Fig. 3A, 3B). In contrast, both the frequency and the number of the $CD8^{neg}$ T/iT cells were significantly reduced in tadpole spleens at 6 dpi, which suggests an egress of this T cell population (Fig. 3C, 3D). Unlike tadpoles, the $CD8^{neg}$ T/iT cell population remained unchanged following *M. marinum* inoculation in the adult spleens (Fig. 3C, 3D).

Similarly, the total number of leukocytes recovered from the liver of *M. marinum*–inoculated adults, but not from tadpoles, significantly increased at 6 dpi, suggesting immune cell influx and/or expansion (Table II). The frequency and number of CD8 T cells peaked at 12 dpi only in adult livers, whereas there were no marked changes in tadpole livers (Fig. 4A, 4B). However, the frequency of $CD8^{neg}$ T/iT cells significantly increased at 12 dpi in tadpole livers, suggesting recruitment of these cell types in the liver (Fig. 4C, 4D). In adult livers, the was a significant drop in the frequency of $CD8^{neg}$ T/iT cells at 6 dpi compared with uninfected controls that did not affect their cell number. Taken together, the data suggest that conventional $CD8^+$ T cell response is elicited mainly in adults, whereas tadpole anti–*M. marinum* T cell response appears to rely more on the recruitment of $CD8^{neg}$ T cells that include iT cells.

Histopathology of M. marinum*–inoculated liver of* X. laevis *adults and tadpoles*

Differences were noted in the histopathologic appearance of the livers between adults and tadpoles (Fig. 5A–H). In the liver of postmortem adult frogs, distinct clusters of epithelioid macrophages, indicative of microgranulomas, were scattered randomly throughout the hepatic parenchyma (Fig. 5A, 5D, black arrows). Detailed examination of these microgranulomas in multiple sections of different animals revealed that they were composed almost exclusively of histiocytic cells suggestive of epithelioid macrophages, as shown in representative sections of Fig. 5A, 5D. Often, the microgranulomas were surrounded by a rim of mononuclear cells with little cytoplasm and darker, more condensed nuclear chromatin, consistent with lymphocytes. The largest lesions included basophilic debris, indicative of a poorly demarcated necrotic zone at the core of the microgranuloma (Fig. 5A).

In tadpoles, only a very small number of tiny epithelioid macrophage clusters were present, usually including distinct melanomacrophages or similar cells with nuclei obscured by melanin (representative shown in Fig. 5G). Unlike adults, the microgranulomas present in tadpoles had no evidence of a necrotic zone. Based on the number of microgranulomas per unit of liver tissue, adult frogs exhibited a significantly higher

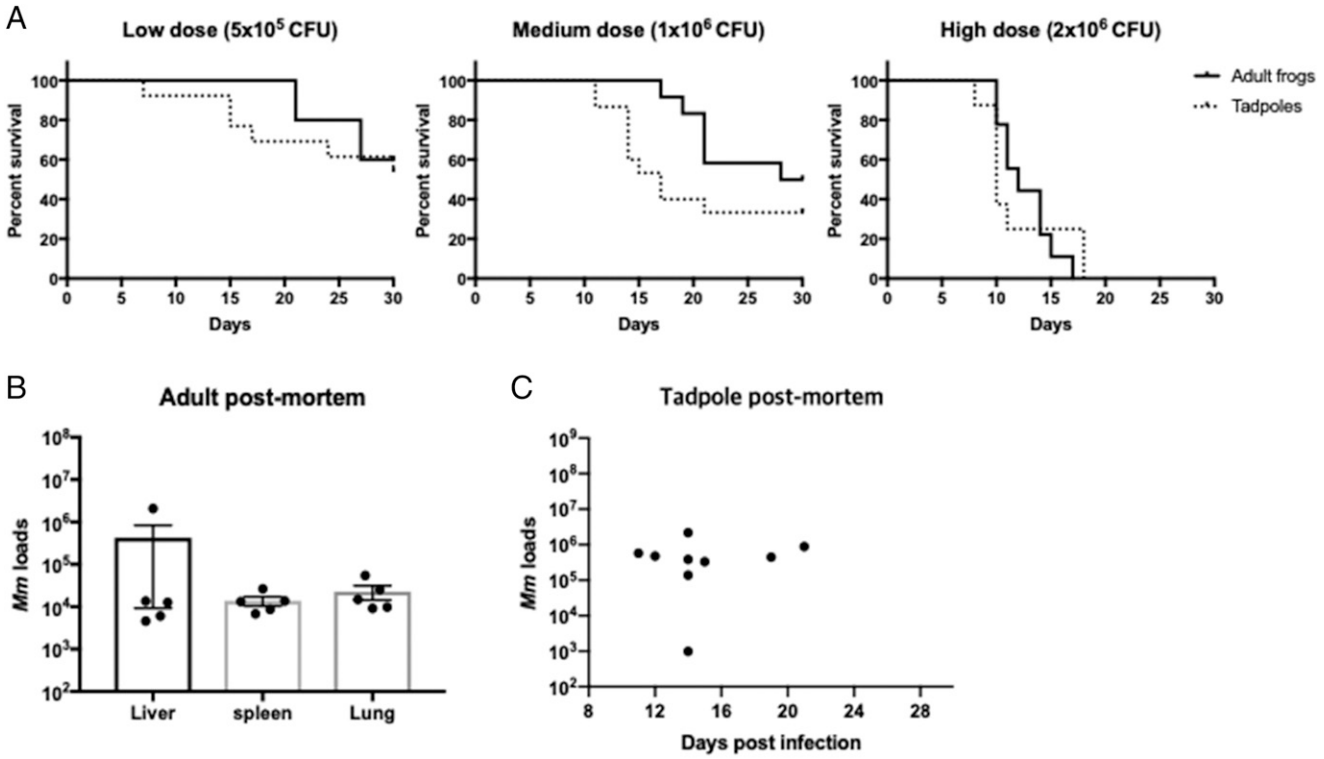

FIGURE 1. Survival curves of *M. marinum*–inoculated adults and tadpoles of *X. laevis*. (**A**) Four-month-old adults (n = 5–10 per group) and 3-wk-old tadpoles (developmental stage of 52, n = 10–19 per group) were inoculated with different amounts of *M. marinum* i.p. (5×10^5 CFU for low dose, 1×10^6 CFU for medium dose, and 2×10^6 CFU for high dose). The survival rate was dependent on the doses of *M. marinum* based on the Cox proportional hazard model analysis ($p < 0.05$). Comparisons of survival rates between adult frogs and tadpoles for each dose, as well as median survival times, are listed in Table II. (**B**) *M. marinum* loads in different organs from postmortem adults. (**C**) *M. marinum* loads of whole individual postmortem tadpoles. Viral loads were determined by real-time PCR using *M. marinum*–specific 16S rRNA gene.

number of granulomas compared with tadpoles (nonparametric two-way ANOVA, $p < 0.001$) (Fig. 5C).

To visualize T cells in relation to granuloma structures, we used a cross-reactive human anti-CD3 Ab (18). Following *M. marinum* inoculation, we detected an accumulation of $CD3^+$ T cells in both adult and tadpole livers (Fig. 5B, 5E, 5H). More specifically, $CD3^+$ T cells were conspicuously present throughout the parenchyma, either individually or forming small clusters. In the livers of *M. marinum*–inoculated adults, the $CD3^+$ T cells were more numerous in the periphery of the microgranulomas (Fig. 5B, 5E, brown staining). In contrast, overall, fewer $CD3^+$ T cells were scattered almost uniformly throughout the hepatic parenchyma with little association with microgranulomas in tadpole livers (Fig. 5H). Although very rare, a few $CD3^+$ T cells were present within the core of microgranulomas in tadpole livers (Fig. 5E).

Special stains for bacteria and acid-fast organisms (Ziehl Neelsen and Fite Faraco, respectively) failed to detect the presence of any microorganisms in tissues from both adults and tadpoles. However, an isH probe for *Mycobacterium* sp. produced amorphous staining in the cytoplasm of random cells in the livers of adults and tadpoles (Fig. 5F, 5I, respectively). Staining was slightly more structured, occasionally forming round vacuoles, in cells within hepatic microgranulomas compared with those scattered in the parenchyma. Subjectively, positive isH staining seemed higher within microgranulomas than in the rest of the tissue. Histological analyses indicated that *M. marinum* were sequestered in microgranulomas, which were larger and rimmed by abundant $CD3^+$ T cells in adult frogs but smaller and less $CD3^+$-rich in tadpoles.

Comparison of M. marinum *dissemination in* X. laevis *adults and tadpoles*

We have previously shown that in tadpoles i.p. inoculated, *M. marinum* accumulates in the liver concomitant with a decrease of pathogen loads among peritoneal leukocytes (PLs) (11). In addition, tadpoles that died at different days post–*M. marinum* inoculation had no marked increase of *M. marinum* loads, which is suggestive of persistent *M. marinum* over time (Fig. 1C). To determine whether *M. marinum* has a distinct dissemination pattern in adult frogs, we quantified *M. marinum* loads in different organs. Following i.p injection of 1×10^6 CFU of *M. marinum* in

Table II. Median survival days for adult frogs and tadpoles infected with different doses of *M. marinum* i.p. (dpi)

Life stage	Doses for i.p. Infection			
	3×10^5 CFU	5×10^5 CFU	1×10^6 CFU	2×10^6 CFU
Adult frogs	N/A	33	29	12
Tadpoles	30	30	17	10
p Value for log-rank test	N/A	0.7164	0.1176	0.9449

N/A, no data.

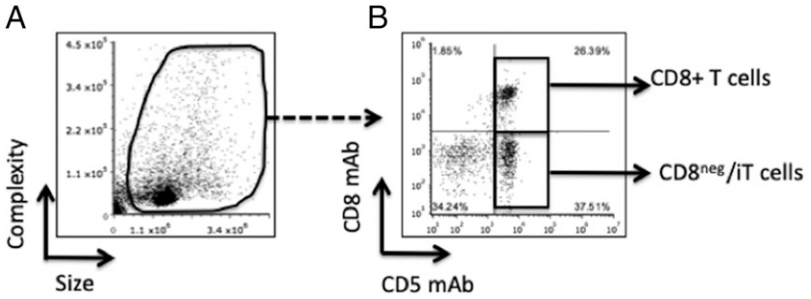

FIGURE 2. Flow cytometric analysis of T cell in spleen and liver of adults and tadpoles. Four-month-old young adults and 3-wk-old tadpoles were i.p. inoculated with 1×10^6 or 3×10^5 CFU of *M. marinum*, respectively (n = 5–6 per time point). Then, the total lymphocytes at different dpi were stained with *Xenopus*-specific CD5 mAb and CD8 mAb to analyze two subsets of T cell populations (**A** and **B**). After gating on live cells, $CD8^+CD5^+$ cells and $CD8^{neg}CD5^+$ cells were defined (black boxes).

adult frogs, we assessed *M. marinum* loads in PLs, which are the first cells to encounter *M. marinum*; the liver, the main site of *M. marinum* dissemination; and the spleen, which is the major lymphoid organ of *X. laevis*.

Similar to tadpoles, we detected persistent *M. marinum* loads among adults' PLs up until 18 dpi, followed by a significant reduction at 21 dpi (Fig. 6A). However, unlike our previously published observation of increased *M. marinum* loads in tadpole livers, we found a significant decrease of *M. marinum* loads in adult livers at 21 dpi (Fig. 6B). In addition, *M. marinum* loads significantly dropped at 18 dpi in the adult spleens (Fig. 6C). Taken together, these data indicate that *M. marinum* disseminates systemically in adult frogs as in tadpoles. Unlike tadpoles, however, *M. marinum* loads significantly decrease in adults' PLs, livers, and spleens over the course of *M. marinum* infection.

Although the absolute quantification assay using qRT-PCR is a highly sensitive method to detect even low *M. marinum* genome copy numbers, the assay does not distinguish live infectious pathogens from dead or inactive *M. marinum*. As a complementary approach, live *M. marinum* from liver tissues were recovered on bacterial culture plates. The CFU of *M. marinum* were measured from infected livers at 21 dpi, which was the time *M. marinum* load decrease was detected in adult frogs by qRT-PCR. Because of the size differences of the liver organs between adults and tadpoles, we normalized the total CFU to milligrams of total tissue lysates. Notably, we detected significantly higher CFU of *M. marinum* in tadpole livers than those of adults at 21 dpi per 1 mg of total protein (Fig. 6D). These data suggest that adult immune responses actively reduce *M. marinum* loads in the adult livers, whereas live *M. marinum* continues to accumulate in the tadpole livers.

Changes in expression profiles of relevant immune genes in the liver

Based on the differences in the histology and the kinetics of *M. marinum* loads between adult frogs and tadpoles, we hypothesized that conventional CD8 T cells and innate immune cells were recruited and actively induced inflammation to control *M. marinum* in adults but not tadpoles. To address this, we determined the relative expression kinetics of genes encoding T cell coreceptors (CD3ε, CD4, and CD8β) as a proxy for recruitment in the liver. We used *gapdh* as a means to normalize the expressions of immune gene transcripts and compared the gene expression profiles between adults and tadpoles. Of note, the Ct value of GAPDH was not markedly different at each time point or between adults and tadpoles (Fig. 7E).

No increase in expression levels of CD3ε, CD4, or CD8β gene was observed in tadpoles following *M. marinum* inoculation (Fig. 7A–C). In contrast, CD8β gene expression was drastically increased (more than 3 logs on average) at 6 dpi in adult liver, consistent with infiltration of conventional CD8 T cells in response to *M. marinum* inoculation (Fig. 7C). To assess the response

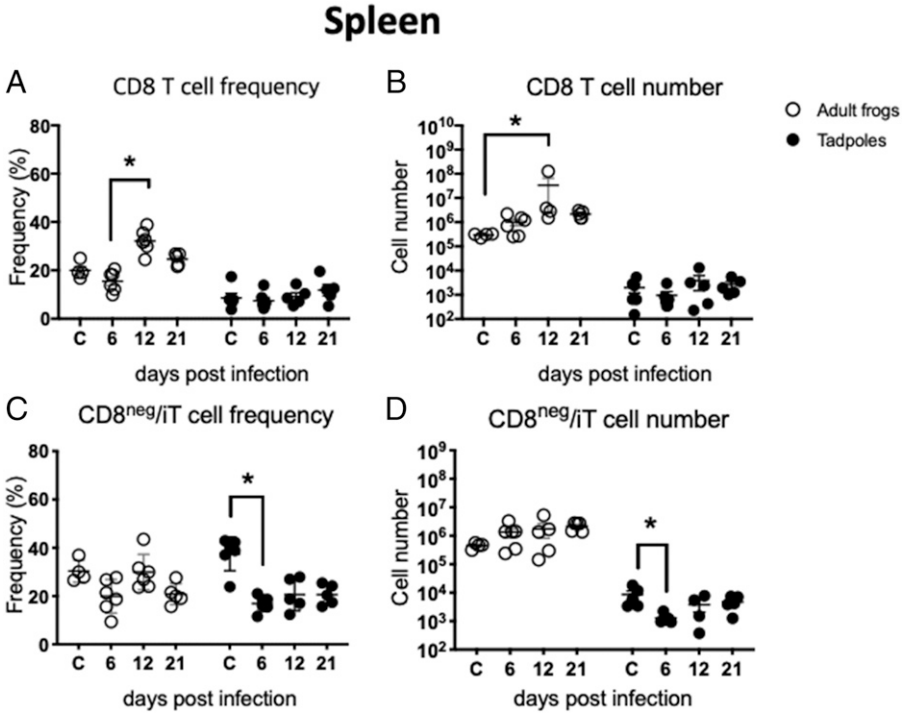

FIGURE 3. Comparison of the frequency and the number of CD8 and $CD8^{neg}$ T/iT cells in the spleen of adults and tadpoles following *M. marinum* inoculation. Using the flow cytometric strategy shown in Fig. 2, the kinetics of CD8 T cell (**A**) frequency and (**B**) number were determined in adults (white) and tadpoles (black) at different days postinoculation (n = 6–7 per group from two independent experiments). Furthermore, the kinetics of $CD8^{neg}$ T/iT cell (**C**) frequency and (**D**) number were determined. Asterisks indicated statistical significance by the Kruskal–Wallis test, nonparametric. C, uninfected control.

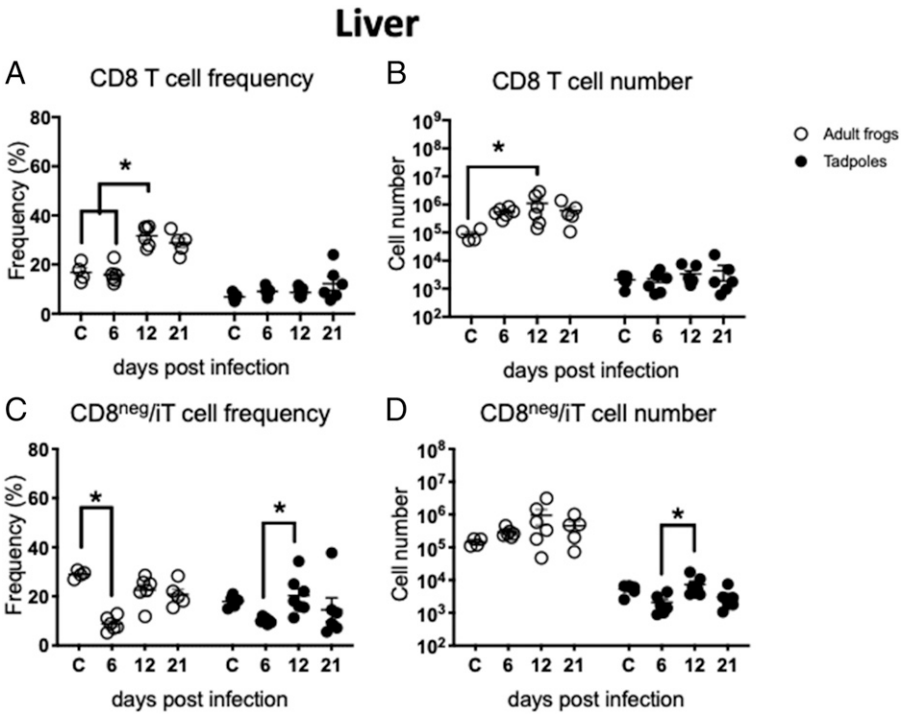

FIGURE 4. Comparison of the frequency and the number of CD8 and $CD8^{neg}$ T/iT cells in the liver of adults and tadpoles during *M. marinum* infection. Using the flow cytometric strategy shown in the Fig. 2, the kinetics of CD8 T cell (**A**) frequency, and (**B**) number were determined in adults (white) and tadpoles (black) at different days postinoculation (n = 6–7 per group from two independent experiments). Furthermore, the kinetics of $CD8^{neg}$ T/iT cell (**C**) frequency and (**D**) number were determined. Asterisks indicated statistical significance by the Kruskal–Wallis test, nonparametric. C, uninfected control.

of iT cells following *M. marinum* inoculation, we determined the transcript levels of the invariant Vα45-Jα1.14 (iVα45-Jα1.14) rearrangement that is expressed by critical anti–M. *marinum* iT cell effectors (10). In tadpoles, iVα45-Jα1.14 transcripts were undetectable in the uninfected livers but became rapidly abundant at 6 dpi and remained detectable at 12 dpi (Fig. 7D). A similar increase in iVα45-Jα1.14 transcript level occurred in the adult livers during *M. marinum* infection. These data support our hypothesis of a dominant anti–*M. marinum* iT cell in tadpoles, contrasting with a combined iT and conventional CD8 T cell response in adult frogs.

To assess the involvement of innate immune cell effectors in adult and tadpole livers during *M. marinum* infection, we monitored the expression of CSF-1R as a marker for macrophages, G-CSF-R as a marker for neutrophils, and CCR2 as a marker for inflammatory monocytes in the liver (Fig. 8A–C). In addition, we determined the expression of proinflammatory and anti-inflammatory cytokine genes (Fig. 8D–H). Notably, CSF-1R gene expression peaked at 6 dpi in adult frogs and returned the basal level at 12 dpi (Fig. 8A). The transcript levels of G-CSF-R and CCR2 did not change at the two time points tested (Fig. 8B, 8C). Interestingly, the increase in CSF-1R expression was correlated with that of TNF-α, IL-1β, and inducible NO synthase, which are proinflammatory cytokines (Fig. 8D–F). We did not find a significant increase of expression of anti-inflammatory cytokines such as TGF-β or IL-10 at 6 and 12 dpi (Fig. 8G, 8H). In tadpoles, we observed a reduced expression of CSF-1R at 12 dpi compared with uninfected tadpoles (Fig. 8A). Although the kinetics of TNF-α, IL-1β, and iNOS did not drastically change in tadpoles, we found that the expression of TGF-β significantly dropped at 12 dpi in parallel to CSF-1R (Fig. 8G). Taken together, these data suggest that the acute influx or activation of macrophages (indicated by CSF-1R) and conventional CD8 T cells (indicated by CD8β cells) may contribute to early inflammation in adult frogs, whereas mainly iT cells (indicated by Vα45-Jα1.14 rearrangement) are recruited and persistent in tadpoles without marked inflammation.

Discussion

The wide range of host species infected by *M. marinum* poses a concern not only for the aquatic ecosystem and fish industry but also for its potential risk to public health. Aquatic species notoriously infected by *M. marinum* include *X. laevis*, which we used in this study as a model to understand host anti–*M. marinum* immune response. Although the immune system of tadpoles is generally considered more immature and/or less efficient in controlling pathogens than that of adult frogs, our study rather suggests a distinct adaptation and specialization of immune responses for each these two life stages in *X. laevis*. Notably, unlike adult frogs that exhibit potent conventional CD8 T cell effectors, tadpoles do not express an optimal level of MHC I protein until the onset of metamorphosis and predominantly rely on immunity driven by MHC I–like and iT cells (8, 11). In this study, we report evidence that suggests a distinctive host–pathogen interaction between adults and tadpoles during *M. marinum* infection.

First, in apparent contradiction of the general view of weaker tadpole immunity, we found a comparable survivorship between

Table III. Total number of lymphocytes ($\times 10^3$) ± SE

Organ	Stage	Control	6 dpi	12 dpi	21 dpi
Spleen	Adult	1500 ± 158	6000 ± 1450	4860 ± 2104	9580 ± 1632, $p = 0.0226$[a]
	Tadpole	24 ± 11	12 ± 4	34 ± 16	22 ± 4
Liver	Adult	505 ± 63	3363 ± 309, $p = 0.0316$[a]	3650 ± 1656	2100 ± 710
	Tadpole	30 ± 4	25 ± 6	44 ± 15	32 ± 15

[a]Compared to control using nonparametric Kruskal–Wallis test followed by Dunn test.

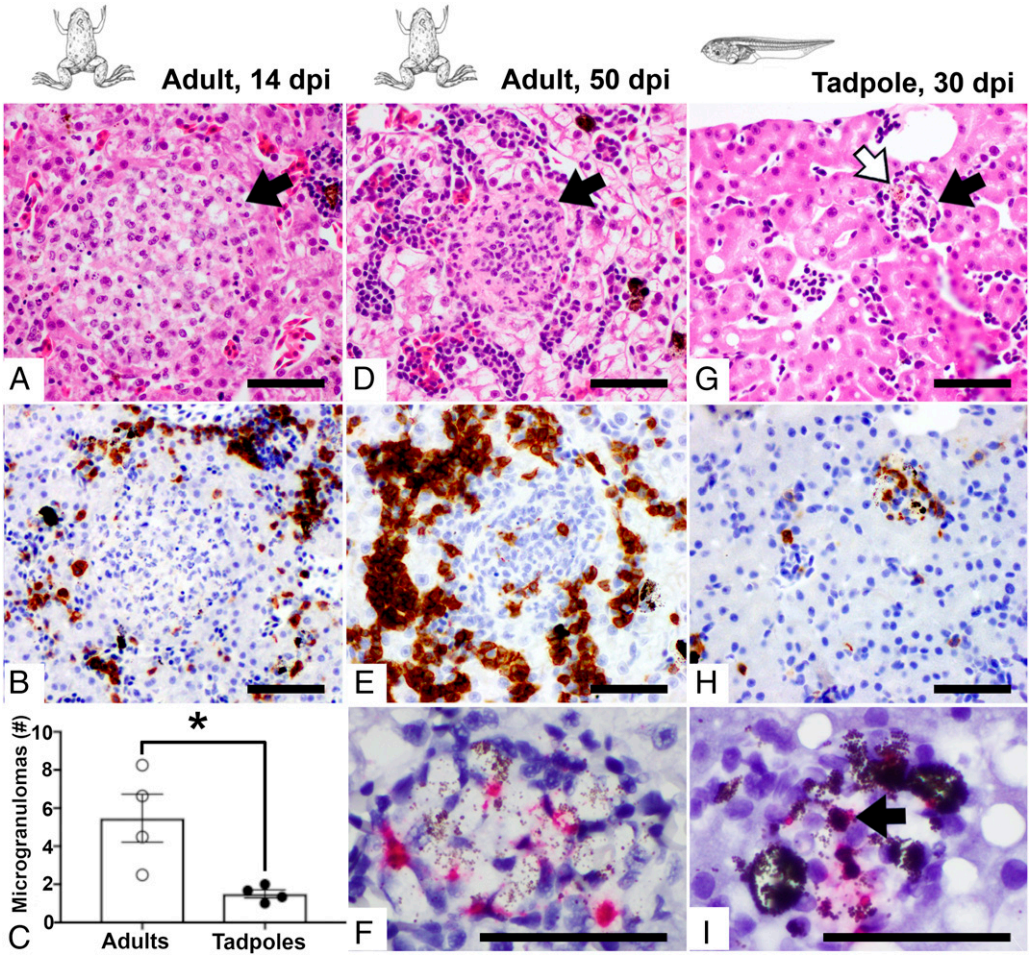

FIGURE 5. Histopathology of the liver of *M. marinum*–inoculated adults and tadpoles and comparison between microgranuloma numbers. Four-month-old young adults and 3-wk-old tadpoles were i.p. inoculated with 1×10^6 or 3×10^5 CFU of *M. marinum*, respectively (n = 5–6 per time point). Representative of liver sections that were stained with H&E (**A**, **D**, and **G**), an anti-CD3 mAb (**B**, **E**, and **H**, brown staining), or an isH (red staining) probe for *Mycobacterium* sp. (**F** and **I**). Adults inoculated with 10^6 CFU of *M. marinum* and euthanized 14 and 50 dpi: Larger granulomas (A and D, black arrows) surrounded by $CD3^+$ cells in moderate (B) to high numbers (E) and positive isH for *Mycobacterium* sp. in the cytoplasm of cells within the granuloma at 50 dpi (F). Tadpole inoculated with 3×10^5 CFU of *M. marinum* and euthanized 30 dpi: Small microgranuloma including cells with intracytoplasmic melanin granules (G, black and white arrows, respectively), with rare $CD3^+$ cells (H) and positive isH for *Mycobacterium* sp. in the cytoplasm of cells within the microgranuloma (I, arrow). Scale bars, 50 μm. The average numbers of microgranulomas in adults at 50 dpi ($n = 4$) were significantly higher than those in tadpoles at 30 dpi ($n = 4$) (**C**). $*p < 0.05$, nonparametric two-way ANOVA.

adults and tadpoles challenged with different doses of *M. marinum*. Considering the smaller size of the tadpoles compared with the adults, the inoculated tadpoles were remarkably efficient in tolerating high amounts of *M. marinum*. This implies that tadpole and adult immune defenses, although distinctive, achieve similar survival against mycobacterial infections. To get further insights into the distinct adaptation of host responses against *M. marinum* by these two life stages, we first examined the T cell response by flow cytometry. Although specific Abs to detect iT and CD4 T cells are currently missing in *Xenopus*, we were able to take advantage of CD5, a pan–T cell marker in *X. laevis*, in combination anti-CD8 mAb to monitor conventional CD8 T cells ($CD8^+/CD5^+$) versus a population of $CD8^{neg}$ T/$CD5^+$ T cells, which have been shown to contain T cells expressing CD4 (21). $CD8^{neg}$ T/$CD5^+$ T cells also include iT cells (e.g., invariant iVα45 [iVα45] T cells) because they express very low levels of CD8 to no CD8 at all (8, 11). Based on this approach, we found that adult frogs exhibit a strong conventional $CD8^+$ T cell response against *M. marinum*, which is not the case in tadpoles, in which the increase of $CD8^{neg}$ T cells and iT cells in the liver, concomitant with their drop in the spleen, suggests their rapid recruitment upon *M. marinum* inoculation. It is noteworthy that splenic IgM^+ B cells are not $CD5^+$ in *X. laevis*, except following strong stimulation with PMA (22). Further investigation by gene expression profiling confirms that *M. marinum* inoculation induces a significant increase of CD8β transcript levels indicative of CD8 T cell response together with iVα45-Jα1.14 mRNAs in the adult liver. In contrast, only increased iVα45-Jα1.14, but not CD8β transcript levels, was detected in tadpoles in response to *M. marinum* inoculation (Fig. 7). It is also interesting to note that CD4 expression significantly decreased, whereas iVα45-Jα1.14 transcript levels remained persistent in *M. marinum*–inoculated tadpole livers (Fig. 7B, 7D). This suggests that iVα45 T cells rather than $CD4^+$ T cells are major effector cells during *M. marinum* infection. This is corroborated by previously published reverse genetic loss-of-function by transgenesis evidence showing that iVα45 cells have a critical host-protective function in tadpoles (10). The mechanisms of activation and functions of these iT cells remain to be elucidated.

A striking difference between adult frogs and tadpoles revealed by this study was the granuloma formation resulting from *M. marinum* inoculation, which consistently occurred in adults but rarely in tadpoles. These granulomas, which consisted of

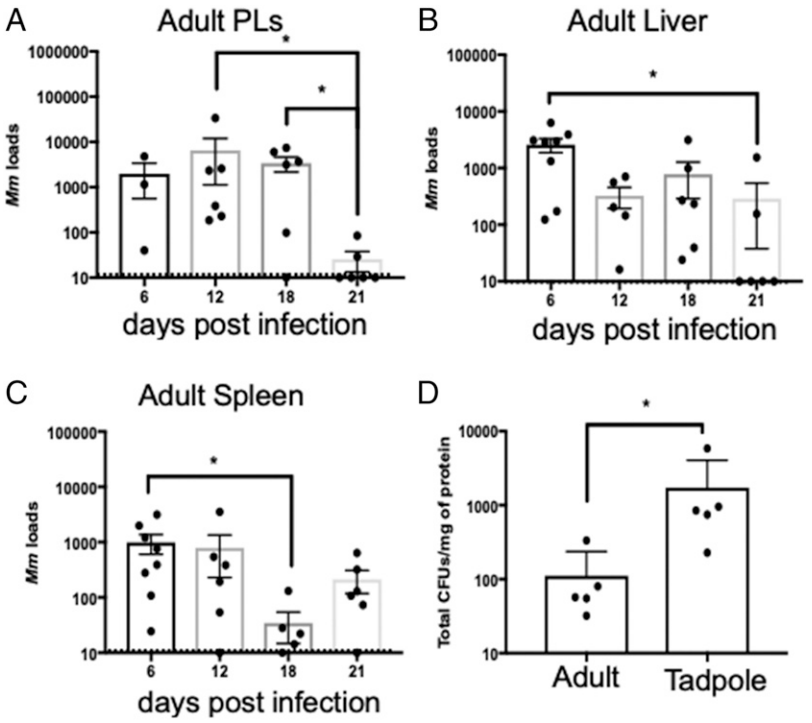

FIGURE 6. Determination of *M. marinum* loads and dissemination using an absolute quantification method and a recovery of live *M. marinum* in culture from adults and tadpoles of *X. laevis*. Adult frogs were i.p. inoculated with 1×10^6 CFU of *M. marinum*, and then *M. marinum* loads were determined using a real-time PCR with *M. marinum*–specific 16S rRNA gene (**A**–**D**). (A) PLs and (B) liver and (C) spleen tissues were taken at the indicated dpi. The dashed line indicates the level of detection by real-time PCR. To measure only the live and replicating *M. marinum*, we cultured kanamycin-resistant *M. marinum* from the inoculated adults and tadpoles at 21 dpi using a Middlebrook 7H10 media supplemented with 50 μg/ml kanamycin. (D) Quantitative measurement of CFU was then normalized to total milligrams of homogenates. Asterisk indicates $p < 0.05$ by Kruskal–Wallis nonparametric test.

epithelioid macrophages surrounded by adaptive T cells, were common in adult liver and, to a lesser extent, in other organs such as lung and spleen. Notably, IHC staining revealed an accumulation of $CD3^+$ T cells at the rim of these granulomas, which is suggestive of a vigorous T cell response against an acute *M. marinum* infection. Histologic examination of the livers of adults and tadpoles occurred at slightly different stages postinoculation, and a definitive conclusion would require further confirmation. However, sampling times included early and late infection for adults and midterm infection in tadpoles. Thus, we believe our findings support an age-dependent difference in immune response. It is uncertain why the special stains that normally pick out mycobacterial organisms failed to do so in the livers of adults or tadpoles. Confirmation of infection was achieved, however, through PCR and culture results and with the positive staining of several cells with an isH probe for *Mycobacterium* sp.

The formation of granulomas is generally associated with inflammation in mammals, especially in cases of mycobacterial infections (23). Likewise, in adult *X. laevis*, the expression of

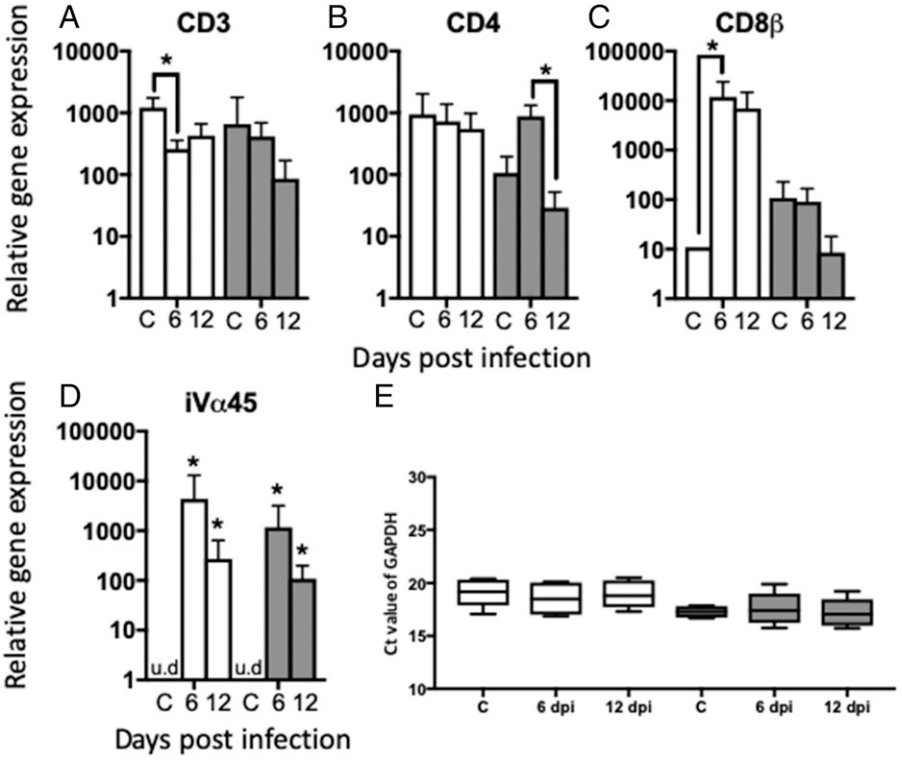

FIGURE 7. Relative expression of T cell–related immune genes in the liver of *M. marinum*–inoculated adults and tadpoles. Four-month-old young adults (white bar) and 3-wk-old tadpoles (gray bar) were i.p. inoculated with 1×10^6 or 3×10^5 CFU of *M. marinum*, respectively (n = 5–6 per time point). Relative gene expression in liver for (**A**) CD3ε, (**B**) CD8β, (**C**) CD4, and (**D**) iVα45-Jα1.14 was normalized to the housekeeping gene *gapdh*. (**E**) Ct values for *gapdh* of each time point between adults and tadpoles. Asterisks indicate a significant difference by the Kruskal–Wallis test ($p < 0.05$). C, uninfected control; u.d, undetected value.

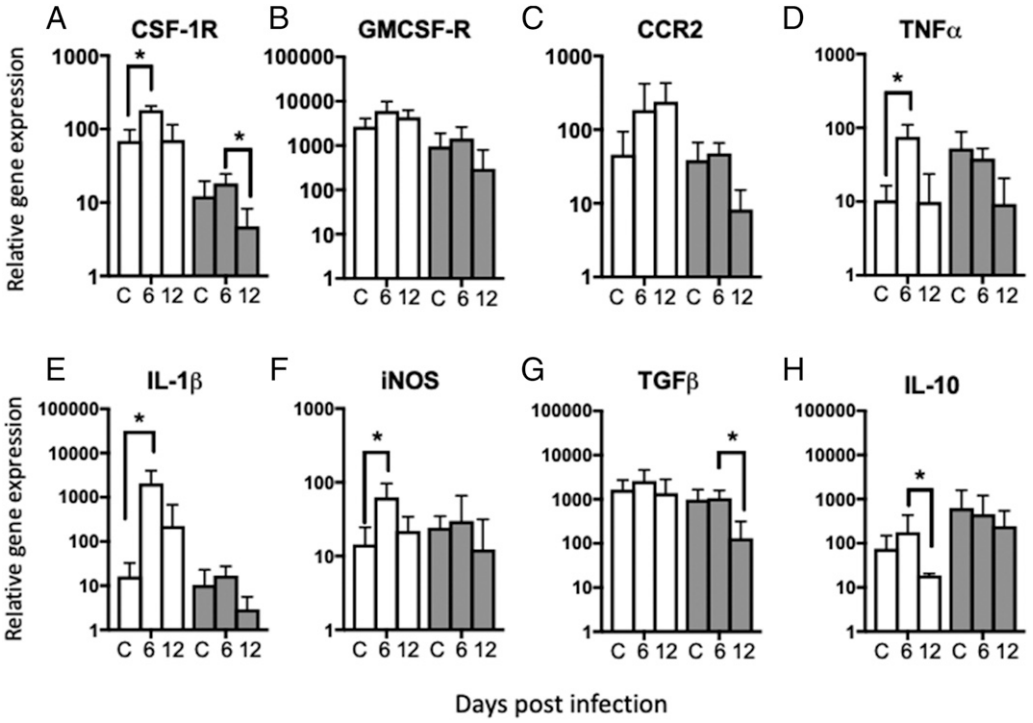

FIGURE 8. Relative expression of immune receptor genes and pro- and anti-inflammatory cytokine genes in the liver of *M. marinum*–inoculated adults and tadpoles. Four-month-old young adults (white bar) and 3-wk-old tadpoles (gray bar) were i.p. inoculated with 1×10^6 or 3×10^5 CFU of *M. marinum*, respectively (n = 5–6 per time point). The relative gene expression in the liver was determined for the immune gene receptors (**A**) CSF-1R (macrophage recruitment marker), (**B**) G-CSF-R (neutrophil recruitment marker), and (**C**) CCR2 (inflammatory monocyte marker); for the proinflammatory cytokine genes (**D**) TNF-α, (**E**) IL-1β, and (**F**) iNOS; and for the anti-inflammatory cytokine genes (**G**) TGF-β and (**H**) IL-10. All the data were normalized to the housekeeping gene *gapdh*. Asterisks indicate significant difference by the Kruskal–Wallis test ($p < 0.05$). C, uninfected control.

several inflammatory genes (TNF-α, IL-1β, and iNOS) was significantly increased following *M. marinum* inoculation in the liver. Collectively, the immune histological analyses further strengthen the critical function of T cells in sequestering and controlling *M. marinum* infection in adult frogs. Importantly, the CD8 T cell–mediated response, inflammation-mediated granuloma formation, and the clearance of *M. marinum* in adult frogs are reminiscent of the critical role of CD8 T cells in granuloma structures of *M. tuberculosis*–infected humans (24). Therefore, our findings suggest that *M. marinum* infection in adult *X. laevis* may complement host mycobacterial infection in mammalian models.

In sharp contrast, microgranulomas were rarely observed in tadpoles (Fig. 3C). In addition, *M. marinum* inoculation did not induce significant expression of inflammatory genes. Indeed, transcript levels of IL-1β remained low following *M. marinum* inoculation, whereas TNF-α or iNOS expression was not induced by *M. marinum.* Importantly, the high CFU counts of live *M. marinum* recovered from the infected livers in this study substantiate the previous report of *M. marinum* accumulation in tadpoles (11). Therefore, it is possible that the dominant iT cell response in tadpoles allows the larval host to tolerate high and persistent *M. marinum* load and, consequently, to maintain the survivorship at a similar level as that of adult frogs. Alternatively, it also possible that the larval $CD8^{neg}$ T cell population includes regulatory T cells (Tregs) that contribute to maintain tolerance to *M. marinum* infection. Although Treg function has not been characterized in amphibians, gene orthologs encoding cytokines and transcription factors critical for differentiation of Tregs (e.g., FOXP3 and CTLA4) are present in the genome of *X. tropicalis* and *X. laevis* (J. Robert, unpublished observations).

From an evolutionary standpoint, it is tempting to speculate that the predominant anti–*M. marinum* iT cell response in tadpoles avoids the activation of inflammation, whereas a conventional T cell response in adults is associated with inflammation. As such, the adaptive host responses against *M. marinum* in two different life stages occupying distinct environmental niches are fundamentally different: the adult conventional T cell–based system is adapted to eradicate *M. marinum* pathogens by killing infected cells and generating an inflammatory response, whereas the tadpole iT cell–based system, upon detection of the infection, is designed to minimize inflammation and tolerate pathogen burden. Consistent with these contrasted immune responses, live *M. marinum* recovered from tadpole livers did not markedly decrease during infection, whereas it decreased in adults. The high *M. marinum* loads found in the adults' postmortem tissues by qPCR further suggest an insufficient clearance of *M. marinum* resulting in the death of the adult frogs.

Active tolerance to pathogen has been reported in various cases, including mycobacterial infection (25–27) Although not as well-defined as immune mechanisms behind host resistance, specific tolerance mechanisms have recently raised attention owing to their relevance for better understanding host–pathogen interactions and potential for developing more effective treatments for infectious diseases. Our data in tadpoles are consistent with an adapted tolerance to *M. marinum* infection that may involve iT cells as specific effectors controlling this tolerance. It will be interesting to examine in more detail how iT cells can establish and control host tolerance to *M. marinum* in tadpoles by determining the specificity (e.g., ligands presented by MHC-like molecules and recognized by iT cells) and the mechanisms involved (e.g., cytokine produced and cell types targeted).

Acknowledgments

We thank Tina Martin for the expert animal husbandry.

Disclosures

The authors have no financial conflicts of interest.

References

1. Tobin, D. M., and L. Ramakrishnan. 2008. Comparative pathogenesis of *Mycobacterium* marinum and *Mycobacterium tuberculosis*. *Cell. Microbiol.* 10: 1027–1039.
2. Franco-Paredes, C., L. A. Marcos, A. F. Henao-Martínez, A. J. Rodríguez-Morales, W. E. Villamil-Gómez, E. Gotuzzo, and A. Bonifaz. 2018. Cutaneous mycobacterial infections. *Clin. Microbiol. Rev.* 32: e00069-18.
3. Hashish, E., A. Merwad, S. Elgaml, A. Amer, H. Kamal, A. Elsadek, A. Marei, and M. Sitohy. 2018. *Mycobacterium* marinum infection in fish and man: epidemiology, pathophysiology and management; a review. *Vet. Q.* 38: 35–46.
4. Cosma, C. L., D. R. Sherman, and L. Ramakrishnan. 2003. The secret lives of the pathogenic mycobacteria. *Annu. Rev. Microbiol.* 57: 641–676.
5. Cronan, M. R., and D. M. Tobin. 2014. Fit for consumption: zebrafish as a model for tuberculosis. *Dis. Model. Mech.* 7: 777–784.
6. Session, A. M., Y. Uno, T. Kwon, J. A. Chapman, A. Toyoda, S. Takahashi, A. Fukui, A. Hikosaka, A. Suzuki, M. Kondo, et al. 2016. Genome evolution in the allotetraploid frog Xenopus laevis. *Nature* 538: 336–343.
7. Robert, J., and Y. Ohta. 2009. Comparative and developmental study of the immune system in Xenopus. *Dev. Dyn.* 238: 1249–1270.
8. Edholm, E. S., L. M. Albertorio Saez, A. L. Gill, S. R. Gill, L. Grayfer, N. Haynes, J. R. Myers, and J. Robert. 2013. Nonclassical MHC class I-dependent invariant T cells are evolutionarily conserved and prominent from early development in amphibians. *Proc. Natl. Acad. Sci. USA* 110: 14342–14347.
9. Edholm, E. S., L. Grayfer, F. De Jesús Andino, and J. Robert. 2015. Nonclassical MHC-restricted invariant Vα6 T cells are critical for efficient early innate antiviral immunity in the Amphibian Xenopus laevis. *J. Immunol.* 195: 576–586.
10. Edholm, E. S., M. Banach, K. Hyoe Rhoo, M. S. Pavelka, Jr., and J. Robert. 2018. Distinct MHC class I-like interacting invariant T cell lineage at the forefront of mycobacterial immunity uncovered in *Xenopus*. *Proc. Natl. Acad. Sci. USA* 115: E4023–E4031.
11. Le Bourhis, L., E. Martin, I. Péguillet, A. Guihot, N. Froux, M. Coré, E. Lévy, M. Dusseaux, V. Meyssonnier, V. Premel, et al. 2010. Antimicrobial activity of mucosal-associated invariant T cells. [Published erratum appears in 2010 *Nat. Immunol.* 11: 969.] *Nat. Immunol.* 11: 701–708.
12. Huang, S. 2016. Targeting innate-like T cells in tuberculosis. *Front. Immunol.* 7: 594.
13. Hyoe, R. K., and J. Robert. 2019. A *Xenopus* tadpole alternative model to study innate-like T cell-mediated anti-mycobacterial immunity. *Dev. Comp. Immunol.* 92: 253–259.
14. Zahn, N., M. Levin, and D. S. Adams. 2017. The Zahn drawings: new illustrations of *Xenopus* embryo and tadpole stages for studies of craniofacial development. *Development* 144: 2708–2713.
15. Luna, L. G. 1968. *Manual of Histologic Staining Methods of the Armed Forces Institute of Pathology*, 3rd Ed. McGraw-Hill, New York, p. 40–41, 220.
16. Beebe, K. 1984. *A Phenol Crystal Violet Stain for Differential Staining of Gram Positive and Negative Bacteria*, Vol. 8, No. 4, Miles Scientific, Newark, DE, p. 216.
17. Lillie, R. D. 1954. *L., Histologic Technic and Practical Histochemistry.* McGraw-Hill, New York, p. 381.
18. Göbel, T. W., E. L. Meier, and L. Du Pasquier. 2000. Biochemical analysis of the *Xenopus laevis* TCR/CD3 complex supports the "stepwise evolution" model. *Eur. J. Immunol.* 30: 2775–2781.
19. Morales, H. D., and J. Robert. 2007. Characterization of primary and memory CD8 T-cell responses against ranavirus (FV3) in *Xenopus laevis*. *J. Virol.* 81: 2240–2248.
20. Neely, H. R., and M. F. Flajnik. 2016. Emergence and evolution of secondary lymphoid organs. *Annu. Rev. Cell Dev. Biol.* 32: 693–711.
21. Chida, A. S., A. Goyos, and J. Robert. 2011. Phylogenetic and developmental study of CD4, CD8 α and β T cell co-receptor homologs in two amphibian species, Xenopus tropicalis and Xenopus laevis. *Dev. Comp. Immunol.* 35: 366–377.
22. Jürgens, J. B., L. A. Gartland, L. Du Pasquier, J. D. Horton, T. W. Göbel, and M. D. Cooper. 1995. Identification of a candidate CD5 homologue in the amphibian *Xenopus laevis*. *J. Immunol.* 155: 4218–4223.
23. Sasindran, S. J., and J. B. Torrelles. 2011. *Mycobacterium tuberculosis* infection and inflammation: what is beneficial for the host and for the bacterium? *Front. Microbiol.* 2: 2.
24. Lin, P. L., and J. L. Flynn. 2015. CD8 T cells and Mycobacterium tuberculosis infection. *Semin. Immunopathol.* 37: 239–249.
25. McCarville, J. L., and J. S. Ayres. 2018. Disease tolerance: concept and mechanisms. *Curr. Opin. Immunol.* 50: 88–93.
26. Schneider, D. S., and J. S. Ayres. 2008. Two ways to survive infection: what resistance and tolerance can teach us about treating infectious diseases. *Nat. Rev. Immunol.* 8: 889–895.
27. Meunier, I., E. Kaufmann, J. Downey, and M. Divangahi. 2017. Unravelling the networks dictating host resistance versus tolerance during pulmonary infections. *Cell Tissue Res.* 367: 525–536.